Electronic Supplementary Material (ESI) for Metallomics.

Both metal-chelating and free radical-scavenging synthetic pentapeptides as efficient inhibitors of reactive oxygen species generation

G. Csire,[a,b] L. Canabady-Rochelle,[c] M.-C. Averlant-Petit,[a] K. Selmeczi*,[b] L. Stefan*,[a]

[a] Laboratoire de Chimie Physique Macromoléculaire, CNRS UMR7375, Université de Lorraine, 1 rue Grandville, 54000 Nancy, France.

[b] Laboratoire Lorrain de Chimie Moléculaire, CNRS UMR 7053, Université de Lorraine, Faculté des Sciences et Technologies, Boulevard des Aiguillettes, 54506 Vandœuvre-lès-Nancy, France.

[c] Laboratoire Réactions et Génie des Procédés, CNRS UMR 7274, Université de Lorraine, 1 rue Grandville, 54000 Nancy, France.

- Supporting information -

Table of contents:

1. Chemical characterization **p.2**
2. Solution equilibrium studies **p.8**
3. Antioxidant activity assays **p.11**
3.A. Ascorbate test **p.11**
3.B. Nitro-blue tetrazolium (NBT) test **p.12**
3.C. Amplex red assay **p.13**
3.D. Coumarin-3-carboxyilic acid (3-CCA) assay **p.14**

1. CHEMICAL ANALYSIS

1.A. Pentapeptide H_2N-Phe-Asp-Asp-Asp-Lys-OH, FD_3K

Compound H_2N-Phe-Asp-Asp-Asp-Lys-OH was obtained as a white solid (176 mg, 203 µmol, 51% yield).

NMR analysis:

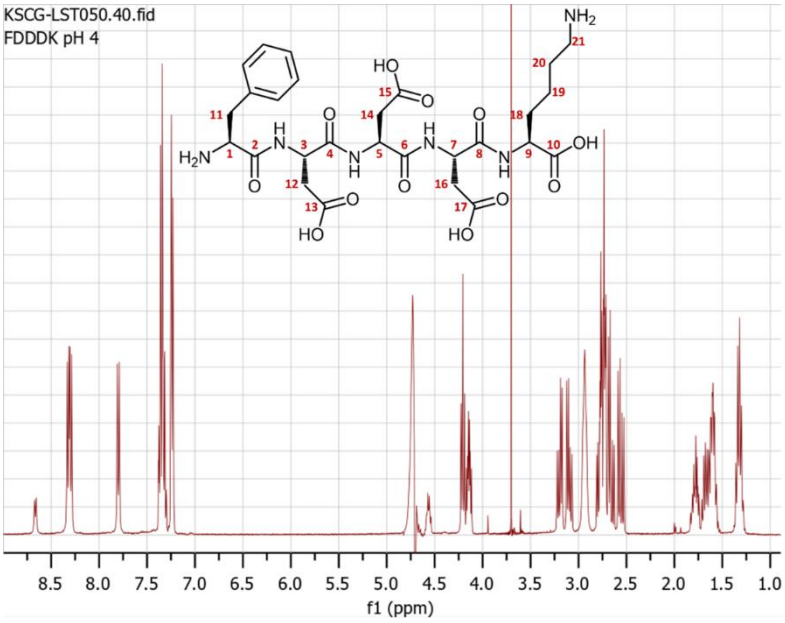

^{1}H NMR (400 MHz, H_2O, pH 4.0) δ (ppm): 1.32 (m, 2H, H19), 1.60 (m, 2H, H20), 1.63-1.84 (m, 2H, H18), 2.52-2.82 (m, 6H, H12, H14, H16), 2.93 (m, 2H, H21), 3.15 (m, 2H, H11), 4.14 (m, 1H, H9), 4.21 (t, *J* = 7.4 Hz, 1H, H1), 4.53-4.60 (m, partially suppressed, H3, H5, H7), 7.21-7.3 (m, 5H, H aromatic), 7.80, 8.31, 8.66 (m, N*H* amide).

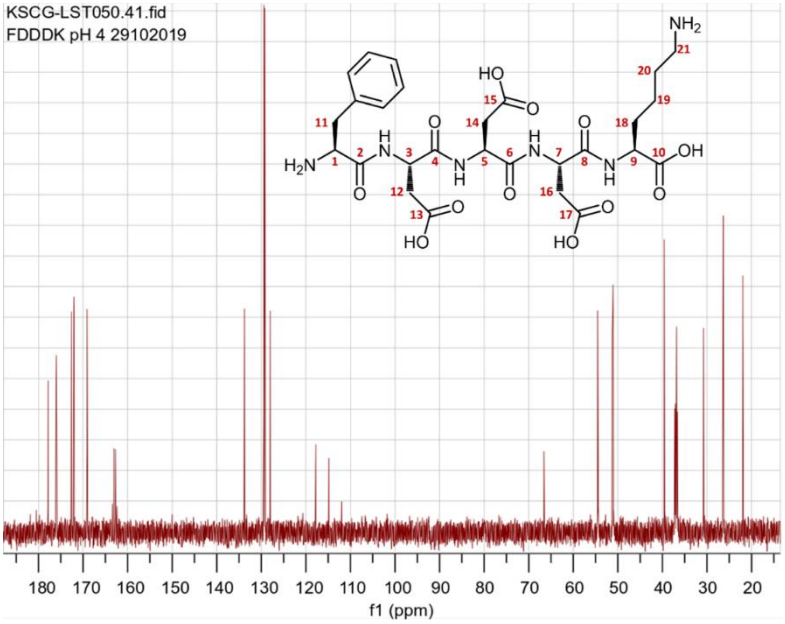

^{13}C NMR (100 MHz, H_2O, pH 4.0) δ (ppm): 21.9 (C19), 26.3 (C20), 30.7 (C18), 36.6, 36.8, 37.1, 37.2 (C12, C14, C16, C11), 39.6 (C21), 51.0, 51.1, 51.2 (C3, C5, C7), 52.8 (C9), 54.1 (C1), 128.0, 129.2, 129.4, 133.8 (C aromatic), 169.1 (C2), 172.0, 172.1 (C4, C6), 172.6 (C8), 175.9, 176.0, 176.1 (C13, C15, C17), 177.8 (C10).

Reverse-phase analytical HPLC chromatogram:

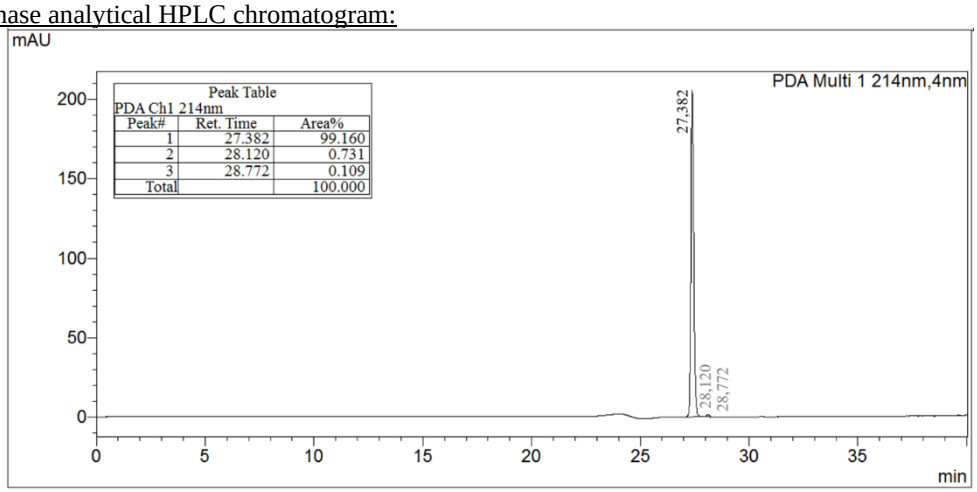

HRMS (ESI): *m/z* calculated for $C_{27}H_{39}N_6O_{12}$ $[M+H]^+$ (100%), 639.2620, found 639.2636.

1.B. Pentapeptide H_2N-Phe-Glu-Glu-Glu-Lys-OH, FE_3K

Compound H_2N-Phe-Glu-Glu-Glu-Lys-OH was obtained as a white solid (257 mg, 283 µmol, 71% yield).

NMR analysis:

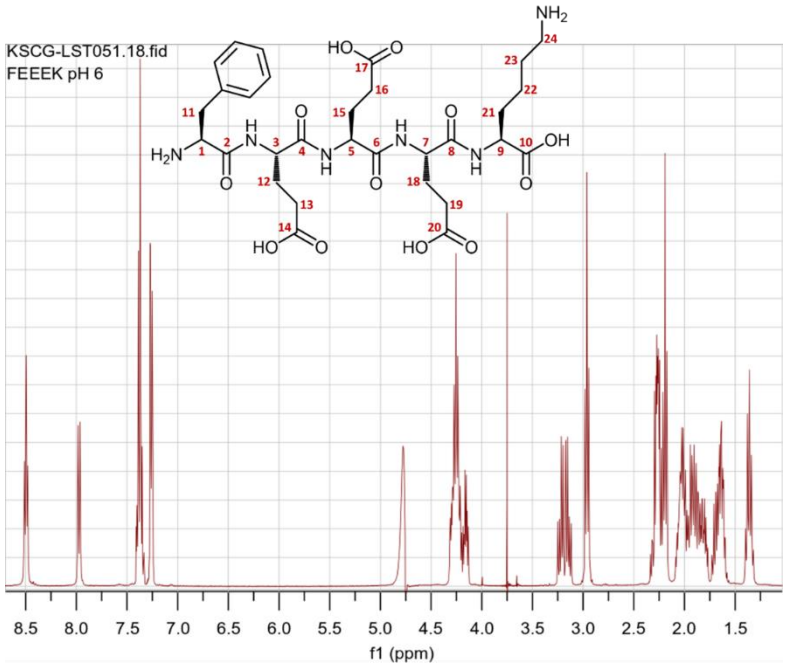

^{1}H NMR (400 MHz, H_2O, pH 6.0) δ (ppm): 1.31 (m, 2H, H22), 1.57 (m, 2H, H23), 1.65 (m, 2H, H21), 1.72-2.04 (m, 6H, H12, H15, H18), 2.14 (m, 2H, H19), 2.23 (m, 4H, H13, H16), 2.91 (t, 2H, H24), 3.13 (m, 2H, H11), 4.10 (m, 1H, H9), 4.21 (m, 1H, H1), 4.15-4.26 (m, 3H, H3, H5, H7), 7.17-7.37 (m, 5H, H aromatic), 7.92, 8.45 (m, N*H* amide).

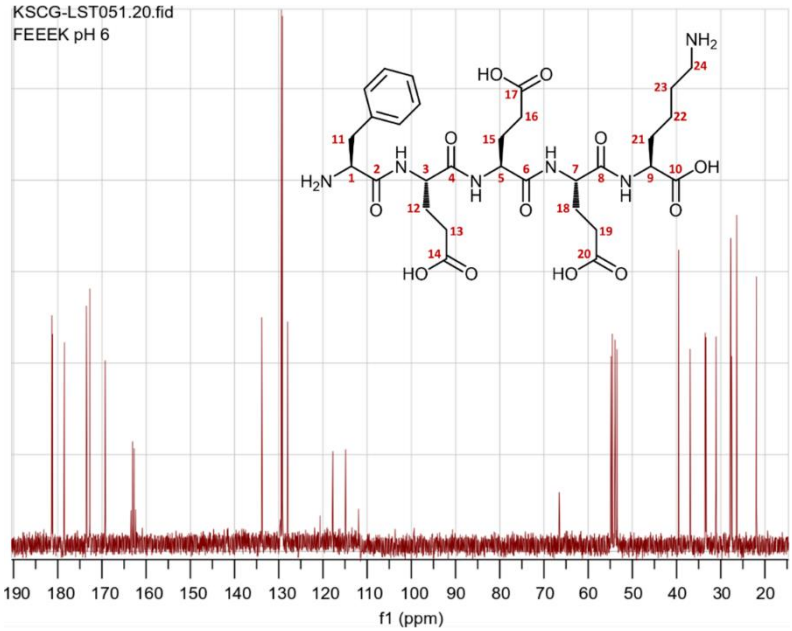

^{13}C NMR (100 MHz, H_2O, pH 6.0) δ (ppm): 22.0 (C22), 26.4 (C23), 27.6 (C18), 27.8 (C12, C15), 31.1 (C21), 33.4 (C19), 33.5, 33.6 (C13, C16), 36.9 (C11), 39.5 (C24), 53.5 (C7), 53.9, 54.0 (C3, C5), 54.6 (C1), 54.8 (C9), 128.0, 129.1, 129.4, 133.8 (C aromatic), 169.3 (C2), 172.6, 172.8 (C4, C6), 173.5 (C8), 178.5 (C10), 181.2 (C20), 181.3, 181.4 (C14, C17).

Reverse-phase analytical HPLC chromatogram:

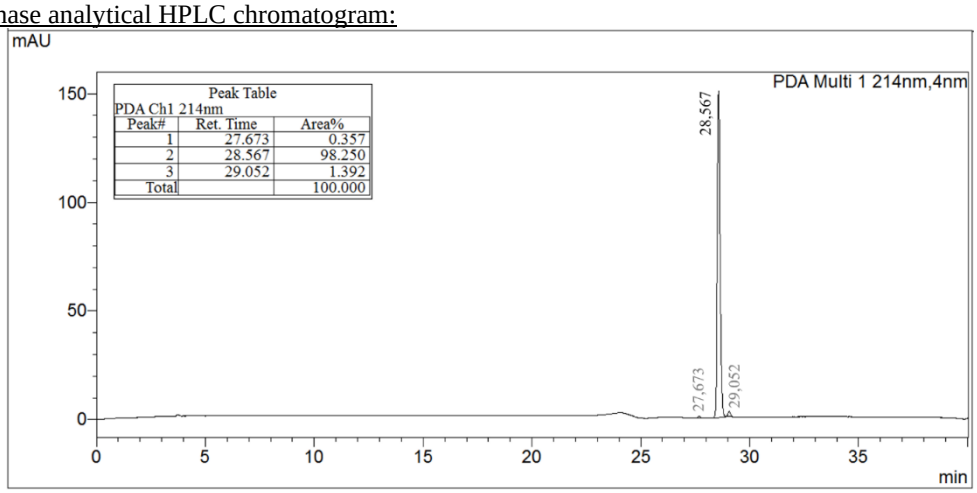

HMRS (ESI): *m/z* calculated for $C_{27}H_{39}N_6O_{12}$ $[M+H]^+$ (100%), 639.2620, found 639.2636.

1.C. Pentapeptide H_2N-Phe-Asp-Asp-Asp-Ala-OH, FD_3A

Compound H_2N-Phe-Asp-Asp-Asp-Ala-OH was obtained as a white solid (162 mg, 233 µmol, 58% yield).

NMR analysis:

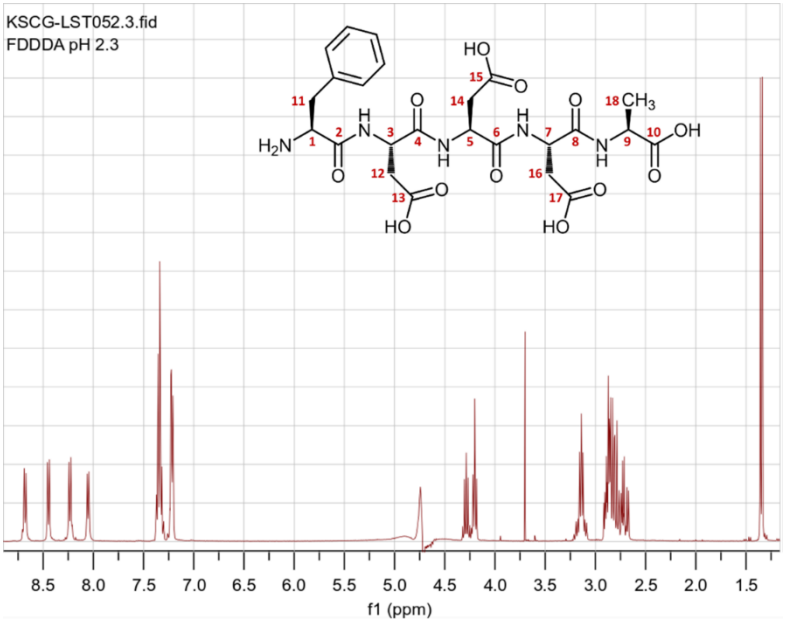

^{1}H NMR (400 MHz, H_2O, pH 2.3) δ (ppm): 1.35 (d, 3H, H18), 2.66-2.92 (m, 6H, H12, H14, H16), 3.14 (m, 2H, H11), 4.21 (t, 1H, H1), 4.29 (m, 1H, H9), 4.25-4.32 (m, 3H, H3, H5, H7), 7.19-7.40 (m, 5H, H aromatic), 8.05, 8.23, 8.44, 8.68 (m, N*H* amide).

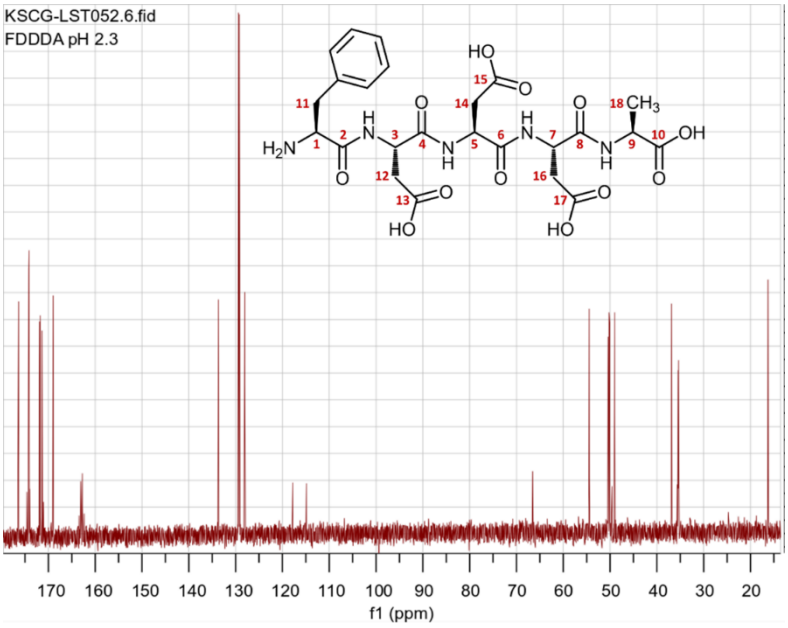

^{13}C NMR (100 MHz, H_2O, pH 2.3) δ (ppm): 16.3 (C18), 35.3-35.5 (C12, C14, C16), 36.9 (C11), 49.0 (C9), 50.1-50.4 (C3, C5, C7), 54.5 (C1), 128.1-133.7 (C aromatic), 169.0 (C2), 171.4-171.9 (C4, C6, C8), 174.1-174.2 (C13, C15, C17), 176.4 (C10).

Reverse-phase analytical HPLC chromatogram:

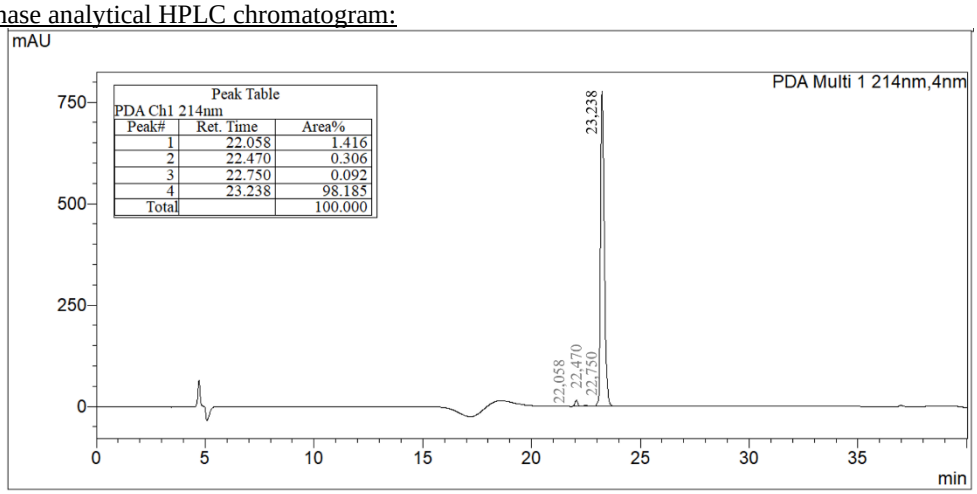

HMRS (ESI): *m/z* calculated for $C_{24}H_{32}N_5O_{12}$ $[M+H]^+$ (100%), 582.2042, found 582.2071.

1.D. Pentapeptide H_2N-Phe-Glu-Glu-Glu-Ala-OH, FE$_3$A

Compound H_2N-Phe-Glu-Glu-Glu-Ala-OH was obtained as a white solid (140 mg, 190 µmol, 48% yield).

NMR analysis:

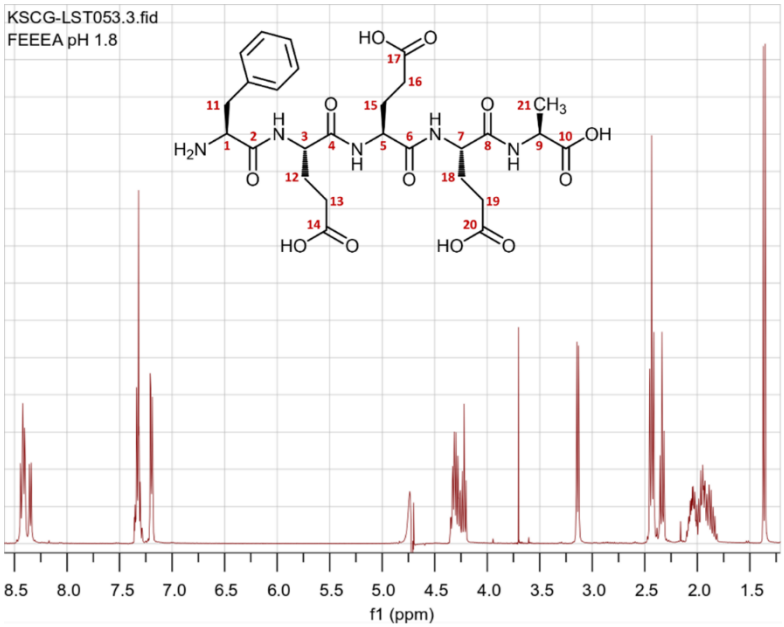

^{1}H NMR (400 MHz, H_2O, pH 1.8) δ (ppm): 1.36 (d, 3H, H21), 1.81-2.11 (m, 6H, H12, H15, H18), 2.34 (t, 2H, H19), 2.43 (t, 4H, H13, H16), 3.14 (d, 2H, H11), 4.22 (t, 1H, H1), 4.25-4.34 (m, 3H, H3, H5, H7), 4.30 (m, 1H, H9), 7.17-7.36 (m, 5H, H aromatic), 8.5-8.46 (m, N*H* amide).

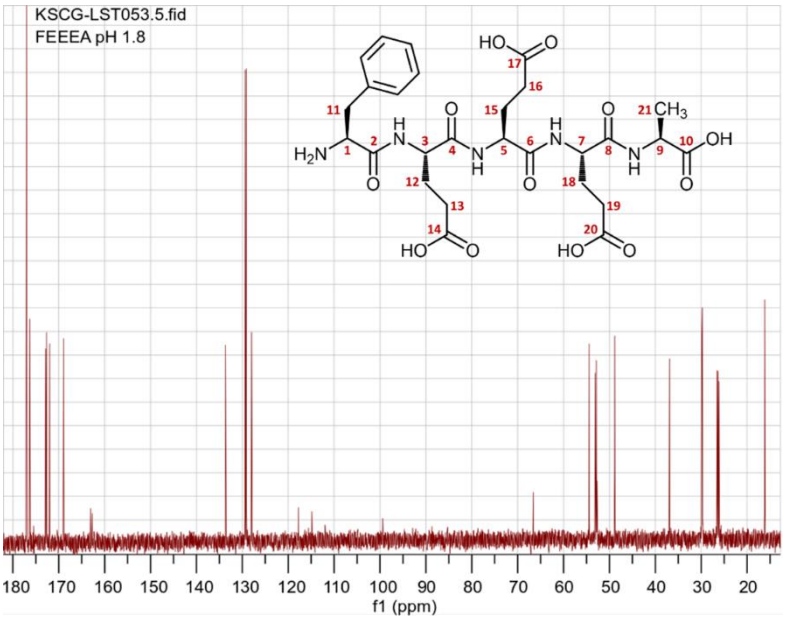

^{13}C NMR (100 MHz, H_2O, pH 1.8) δ (ppm): 16.2 (C21), 26.1-26.3 (C12, C15), 26.5 (C18), 29.7 (C19), 29.8 (C16), 29.8 (C13), 36.9 (C11), 48.9 (C9), 52.7 (C7), 52.9 (C5), 53.1 (C3), 54.4 (C1), 128.0.0-133.6 (C aromatic), 169.0 (C2), 172.0 (C6), 172.7 (C8), 172.9 (C4), 176.4 (C10), 177.0 (C20, C17), 177.1 (C14).

Reverse-phase analytical HPLC chromatogram:

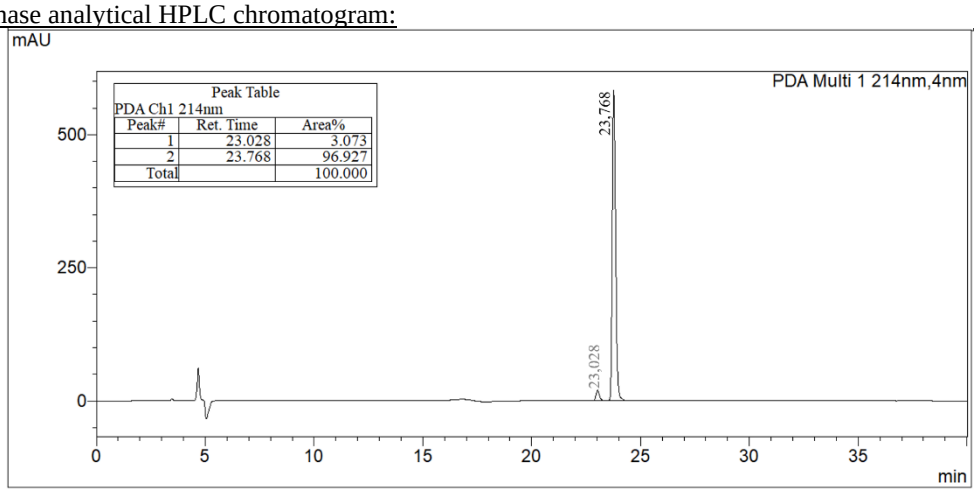

HMRS (ESI): *m/z* calculated for $C_{27}H_{38}N_5O_{12}$ $[M+H]^+$ (100%), 624.2511, found 624.2548.

2. SOLUTION EQUILIBRIUM STUDIES

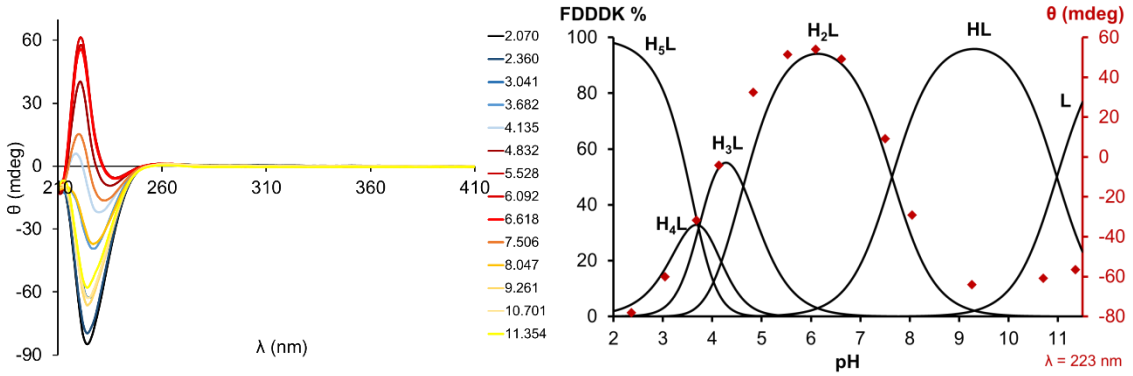

Figure S1. pH dependent CD spectra of FD_3K ligand (left), and pH-dependence of CD signal at 223 nm (right, secondary axis) with the corresponding speciation diagram (right, primary axis). $[FD_3K]_{tot}$ = 1 mM

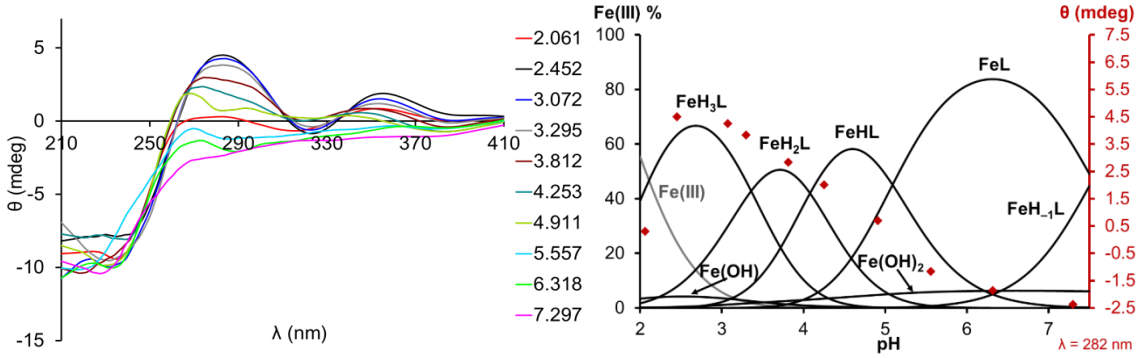

Figure S2. pH dependent CD spectra of FD_3K ligand in the presence of 1 equivalent iron(III) ion (left), and pH-dependence of CD signal at 282 nm (right, secondary axis) with the corresponding speciation diagram (right, primary axis). $[FD_3K]_{tot} = [Fe^{3+}]$ = 1 mM

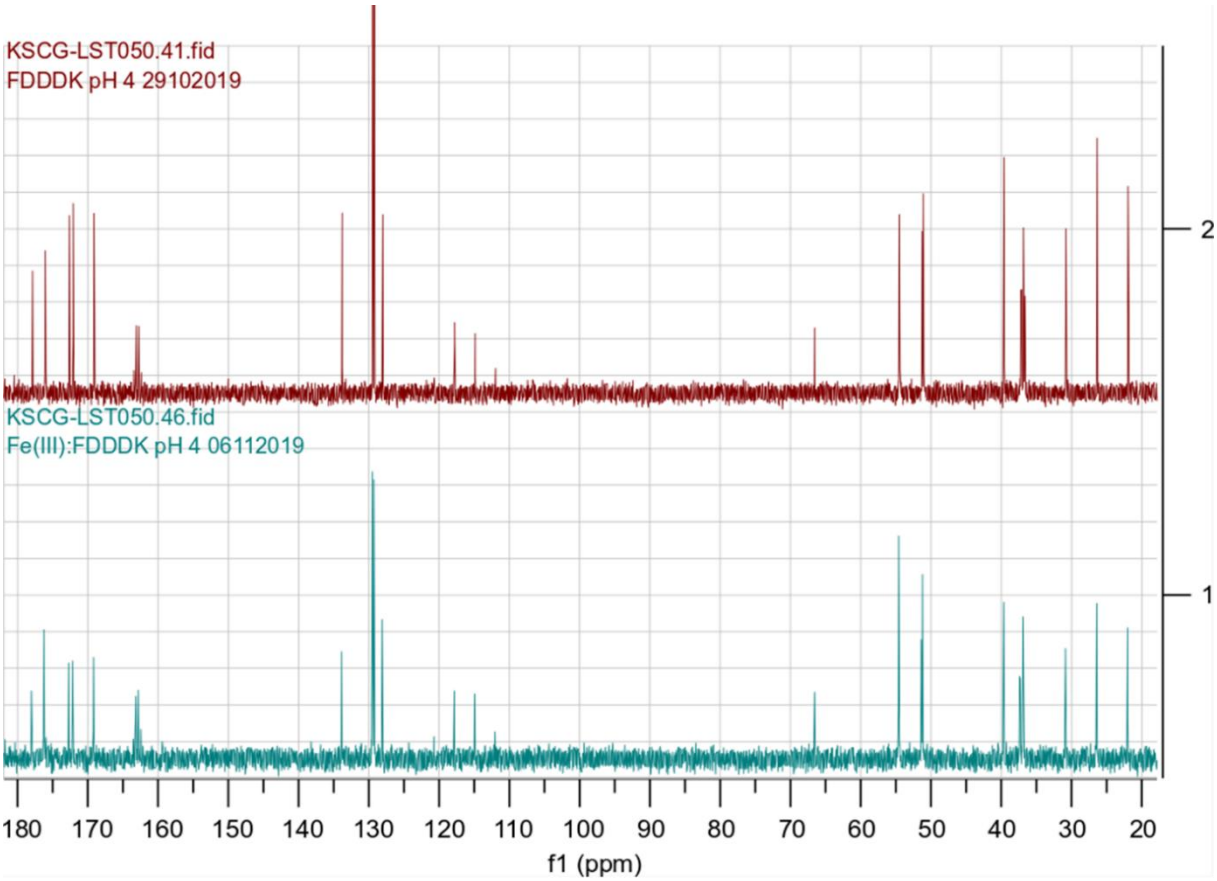

Figure S3. ^{13}C NMR spectra of FD_3K alone (red), complexes Fe(III):FD_3K 1:6 ratio (green) and Fe(III):FE_3K 1:3 ratio (blue) at pH 4

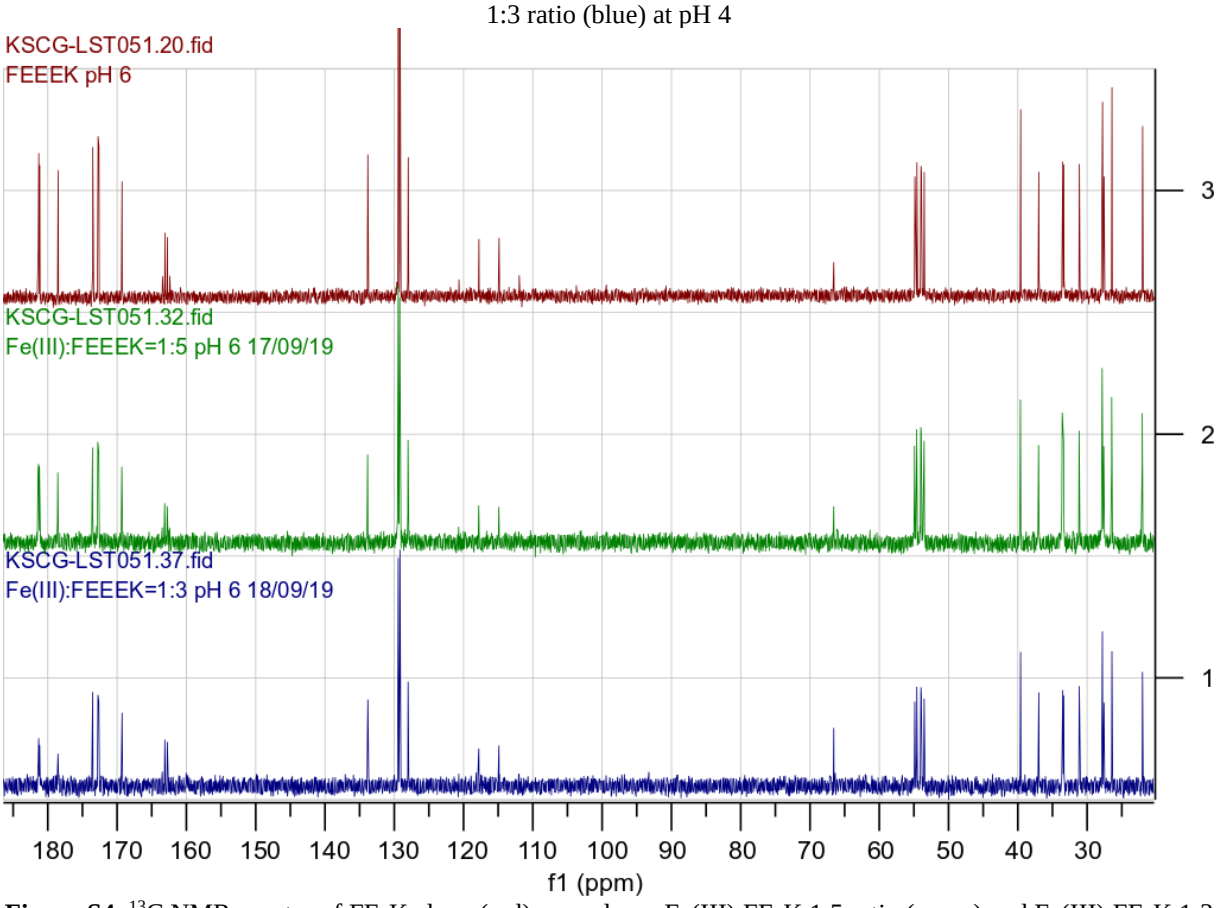

Figure S4. ^{13}C NMR spectra of FE_3K alone (red), complexes Fe(III):FE_3K 1:5 ratio (green) and Fe(III):FE_3K 1:3 ratio (blue) at pH 6.

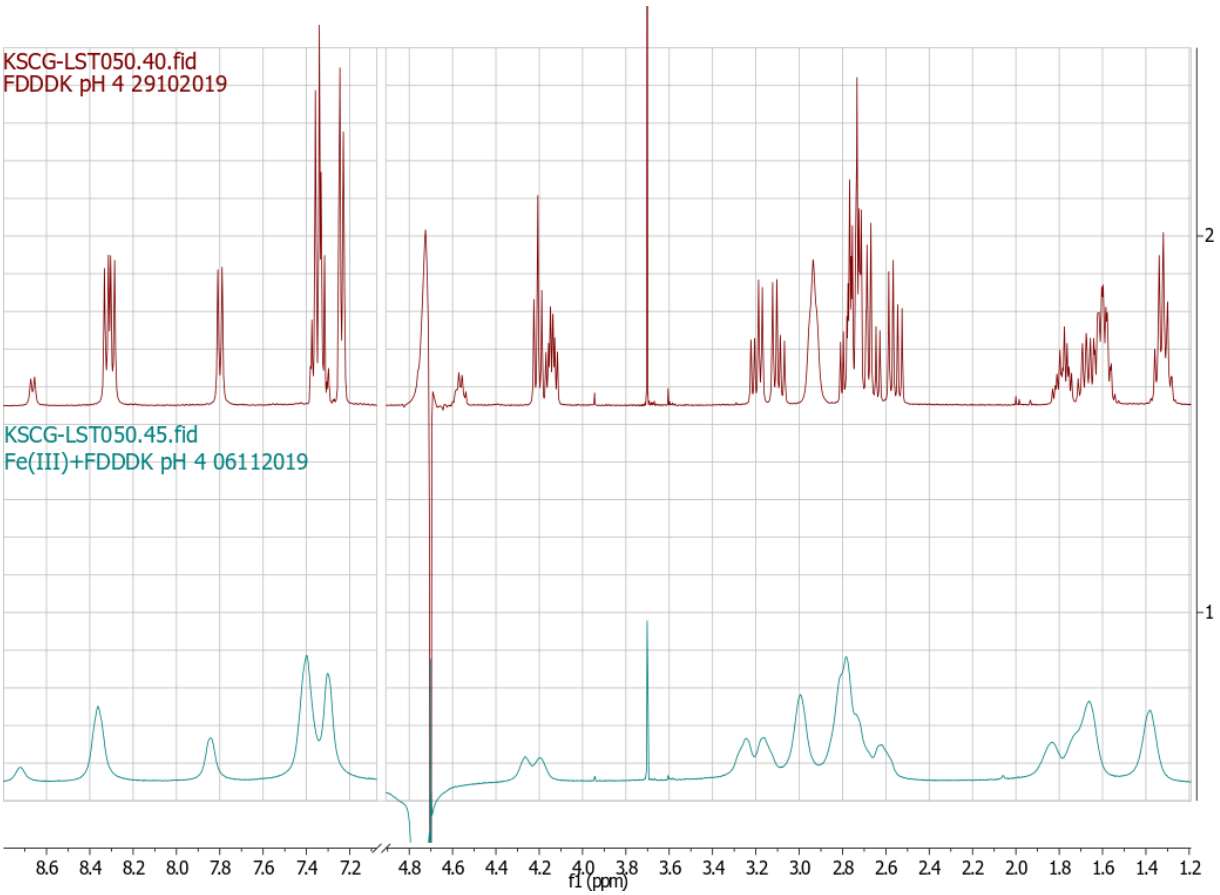

Figure S5. ^{1}H NMR spectra of FD_3K alone (red), complexes Fe(III):FD_3K 1:6 ratio (green) at pH 4.

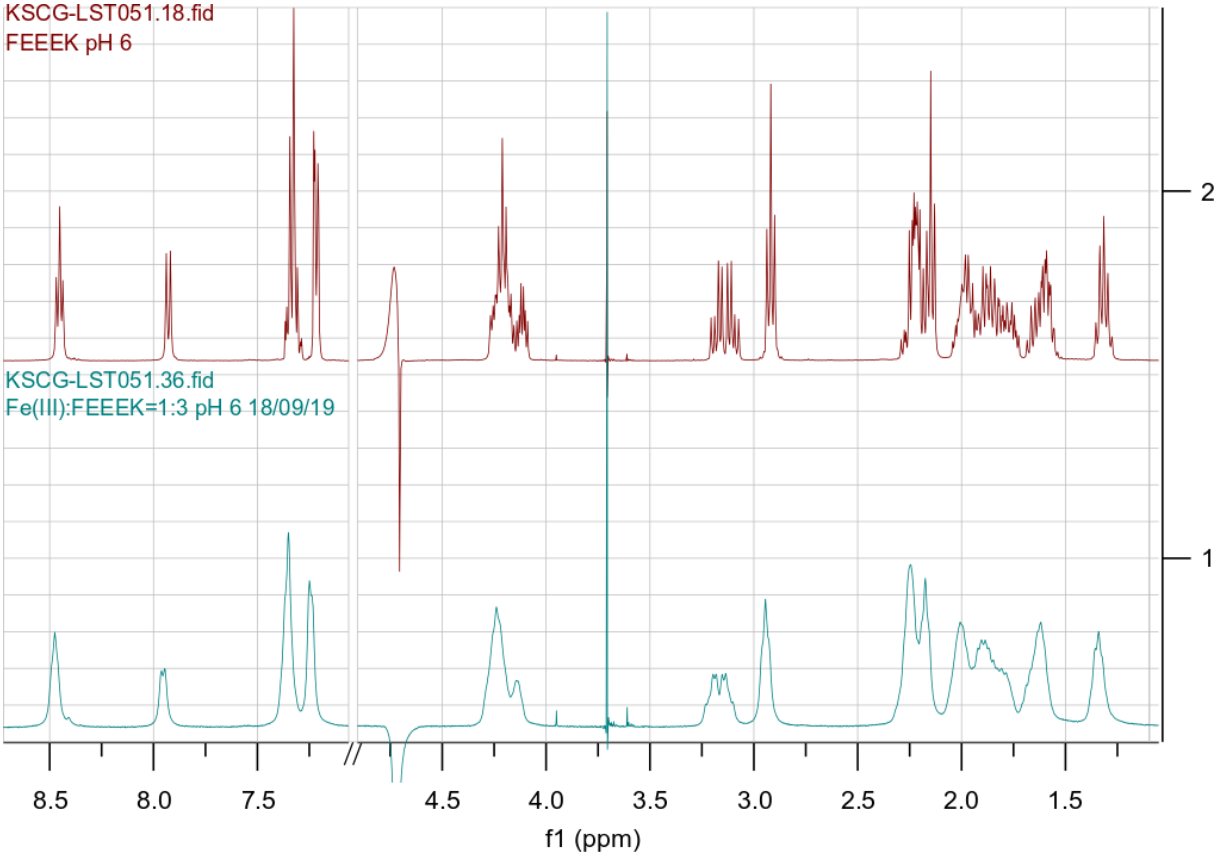

Figure S6. ^{1}H NMR spectra of FE_3K alone (red), complexes Fe(III):FE_3K 1:5 ratio (green) at pH 6.

3. ANTIOXIDANT ACTIVITY ASSAYS

3.A. ASCORBATE TEST

Table S1. Initial reaction rate (standard deviations are in parentheses) and $AscH^-$ concentration after 10 min reaction at pH 6.0 (50 mM MES buffer). $[AscH^-]_0 = [Ligand]_0 = 100$ µM and $[Fe(III)]_0 = 100$ µM if present, $T = 298$ K.

pH 6.0 50 mM MES	$v_i \times 10^{-8}$ (Ms^{-1})	[$AscH^-$] after 10 min (µM)	$AscH^-$ consumed (%)
$AscH^-$	0.14(2)	99.3	0.7
FD_3K	0.088(3)	99.6	0.4
Fe(III):FD_3K	4.4(4)	80.5	19.5
Fe(III):DFO	1.3(2)	93.4	6.6
Fe(III):EDTA	5.70(2)	68.0	32.0
FE_3K	0.10(2)	99.7	0.3
Fe(III):FE_3K	4.1(2)	81.7	18.3

Table S2. Initial reaction rate (standard deviations are in parentheses) and $AscH^-$ concentration after 10 min reaction at pH 7.4 (50 mM HEPES buffer). $[AscH^-]_0 = [Ligand]_0 = 100$ µM and $[Fe(III)]_0 = 100$ µM if present, $T = 298$ K.

pH 7.4 50 mM HEPES	$v_i \times 10^{-8}$ (Ms^{-1})	[$AscH^-$] after 10 min (µM)	$AscH^-$ consumed (%)
$AscH^-$	0.1(1)	99.4	0.6
FD_3K	0.08(3)	99.5	0.5
Fe(III):FD_3K	1.2(2)	92.8	7.2
Fe(III):DFO	0.42(2)	97.5	2.5
Fe(III):EDTA	10.7(4)	35.8	64.2

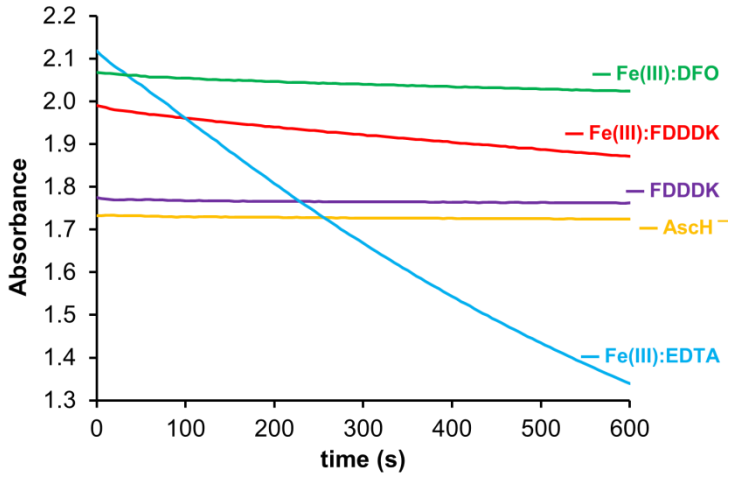

Figure S7. Absorbance at 265 nm *versus* time graph for the ascorbate consumption at pH 7.4 (50 mM HEPES buffer). $[AscH^-]_0 = [Ligand]_0 = 100$ µM and $[Fe(III)]_0 = 100$ µM if present, $T = 298$ K.

3.B. NITRO-BLUE TETRAZOLIUM (NBT) TEST

To measure the quantity of superoxide anion radical formed, the classical NBT test was chosen. The formation of the blue product NBT-diformazan (λ_{max} = 560 nm, ε = 12300 $M^{-1}cm^{-1}$, Scheme S1) was followed spectrophotometrically (see C. Beauchamp and I. Fridovich, *Anal. Biochem.*, 1971, **44**, 276-287). In a general test reaction the following conditions were used: $[AscH^-]_0$ = 300 µM, $[Ligand]_0$ = 100 µM, $[Fe(III)]_0$ = 100 µM and [NBT] = 500 µM in 50 mM buffer solution. Two major problems have been identified during the control measurements: inadequacy of generally used buffers (HEPES and MES) and the reaction between $AscH^-$ and NBT (see K. Reybier, S. Ayala, B. Alies, J. V. Rodriguez, S. B. Rodriguez, G. La Penna, F. Collin, C. M. Gomes, C. Hureau and P. Faller, Angew. Chem. Int. Ed., 2015, 55, 1085-1089). Other buffers, TRIS or phosphate have also been tested and discarded due to the radical scavenging capacity in the case of TRIS, and the strong iron(III) complexation ability in the case of phosphate buffer at a concentration level of 50 mM. Secondly, the reaction between NBT and $AscH^-$ is significant and depends on the pH and the concentration of $AscH^-$ as shown in Figure S5. Because of these interfering side effects, the NBT test was discarded.

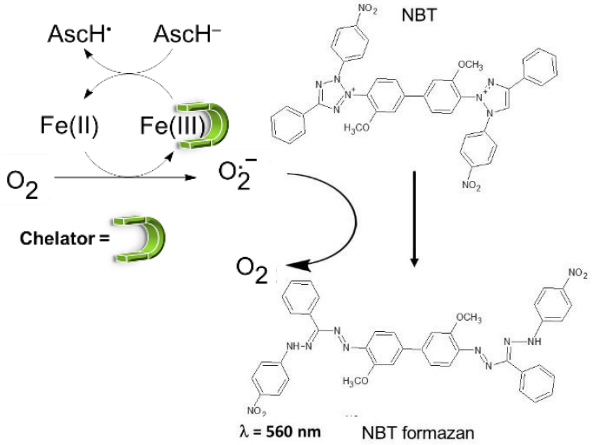

Scheme S1. Reaction between NBT and superoxide anion radical ($O_2^{\bullet -}$).

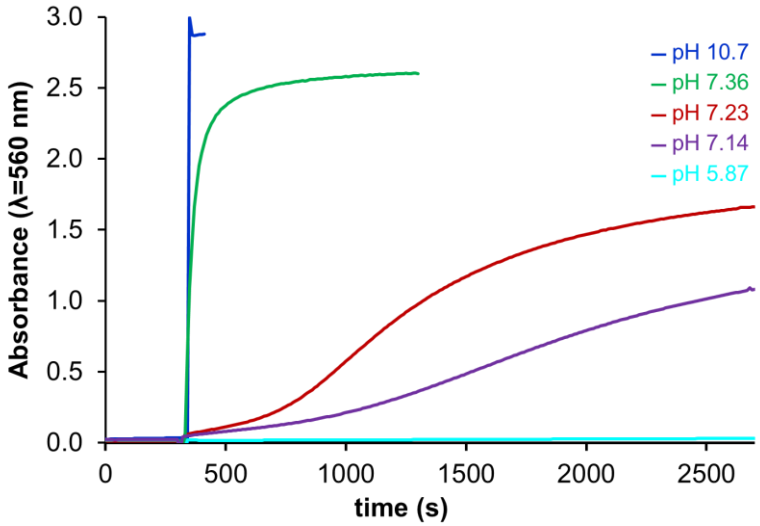

Figure S8. The formation of NBT-diformazan followed at 560 nm as a function of time, showing the pH dependence of the reaction between NBT and $AscH^-$.
$[AscH^-]_0$ = 300 µM and [NBT] = 500 µM in water (pH was adjusted by addition of 0.1 M NaOH).

3.C. AMPLEX RED ASSAY

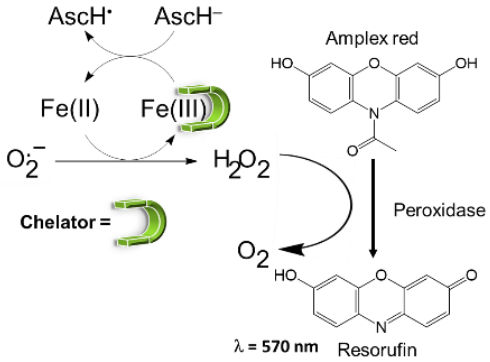

Scheme S2. Reaction between Amplex Red and H_2O_2.

Table S3. Formed H_2O_2 concentrations (standard deviations are in parentheses) after 45 min reaction at pH 6.0 (50 mM MES buffer or water). $[AscH^-]_0$ = 200 µM, $[Ligand]_0$ = 50 µM and $[Fe(III)]_0$ = 50 µM, T = 298 K.

	pH 6.0 in MES		pH 6.0 in water	
	$[H_2O_2]$ (µM)	Formed H_2O_2 / complex ratio (%)	$[H_2O_2]$ (µM)	Formed H_2O_2 / complex ratio (%)
Fe(III):FD_3K	0.9(3)	1.8	2.0(2)	4.0
Fe(III):FE_3K	1.1(2)	2.2	1.8(2)	3.6
Fe(III):EDTA	9.5(6)	19.0	16.7(4)	33.4
Fe(III):DFO	2.3(3)	4.6	1.9(2)	3.8

Table S4. Formed H_2O_2 concentrations (standard deviations are in parentheses) after 45 min reaction at pH 7.4 (50 mM HEPES buffer or water). $[AscH^-]_0$ = 200 µM, $[Ligand]_0$ = 50 µM and $[Fe(III)]_0$ = 50 µM, T = 298 K.

	pH 7.4 in HEPES		pH 7.4 in water	
	$[H_2O_2]$ (µM)	Formed H_2O_2 / complex ratio (%)	$[H_2O_2]$ (µM)	Formed H_2O_2 / complex ratio (%)
Fe(III):FD_3K	0.87(9)	1.8	1.2(1)	2.3
Fe(III):EDTA	7.0(8)	14.0	8.2(2)	16.4
Fe(III):DFO	0.81(4)	1.6	1.9(3)	3.8

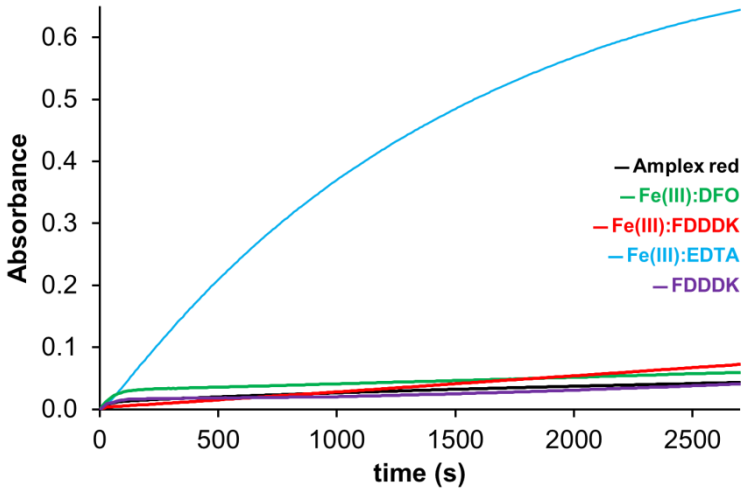

Figure S9. Absorbance at 570 nm *versus* time graph for the H_2O_2 formation at pH 7.4 (50 mM HEPES buffer). $[AscH^-]_0$ = 200 µM, $[Ligand]_0$ = 50 µM and $[Fe(III)]_0$ = 50 µM, T = 298 K.

3.D. COUMARIN-3-CARBOXYILIC ACID (3-CCA) ASSAY

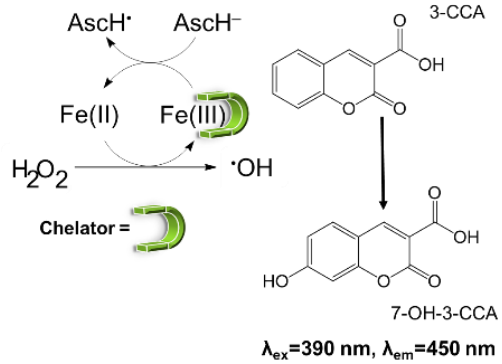

Scheme S3. Reaction between 3-CCA and hydroxyl radical (HO•).

Table S5. Formed HO• concentrations (standard deviations are in parentheses) after 30 min reaction at pH 6.0 and 7.4 in water. $[AscH^-]_0$ = 125 μM, $[Ligand]_0$ = 50 μM and $[Fe(III)]_0$ = 50 μM in the case of peptides (FD_3K, FE_3K) and DFO. $[AscH^-]_0$ = 12.5 μM, $[Ligand]_0$ = 5.0 μM and $[Fe(III)]_0$ = 5.0 μM in the case of EDTA, T = 298 K.

	pH 6.0 in water		pH 7.4 in water	
	[HO•] (μM)	Formed HO•/ complex ratio (%)	[HO•] (μM)	Formed HO•/ complex ratio (%)
Fe(III):FD_3K	0.033(2)	0.07	0.25(1)	0.50
Fe(III):FE_3K	0.051(2)	0.10	-	-
Fe(III):EDTA	0.31(4)	6.20	0.48(6)	9.60
Fe(III):DFO	0.062(5)	0.12	0.07(1)	0.14

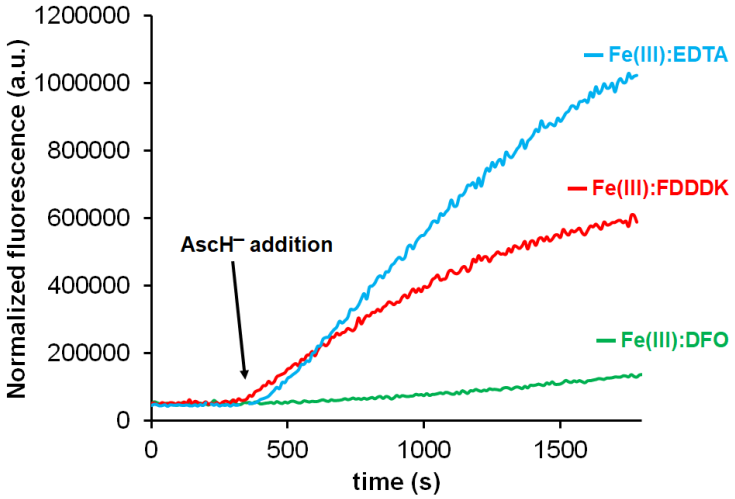

Figure S10. Normalised emission at 450 nm (λ_{ex} = 395 nm) *versus* time graph for the HO• radical formation at pH 7.4 in water. $[AscH^-]_0$ = 125 μM, $[Ligand]_0$ = 50 μM and $[Fe(III)]_0$ = 50 μM in the case of FD_3K and DFO. $[AscH^-]_0$ = 12.5 μM, $[Ligand]_0$ = 5.0 μM and $[Fe(III)]_0$ = 5.0 μM in the case of EDTA, T = 298 K.